

Silicon nitride waveguide-integrated Ge/SiGe quantum wells optical modulator

Papichaya Chaisakul^{1,2*}, Vladyslav Vakarin¹, Jacopo Frigerio³, Giovanni Isella³,
Laurent Vivien¹ and Delphine Marris-Morini¹

¹ Centre de Nanosciences et de Nanotechnologies, Bât 220, rue André Ampère -
Université Paris-Sud, CNRS, 91405 Orsay cedex, France

² Department of Physics, Faculty of Science, Kasetsart University, Bangkok, 10900
Thailand

³ L-NESS, Dipartimento di Fisica del Politecnico di Milano, Polo di Como, Via
Anzani 42, I 22100 Como, Italy

*fscipac@ku.ac.th

Abstract. Silicon-based photonics has generated a strong interest in recent years, mainly for optical interconnects and sensing on photonic integrated circuits. The main rationales of silicon photonics are the reduction of energy consumption and photonic system costs via integration on a standard Si chip. Waveguide-integrated silicon based-optoelectronic modulators have been particularly studied as a key building block. Ge-rich Ge/SiGe quantum well waveguides are promising for compact and low energy consumption modulators thanks to the demonstration of direct gap related optical transitions in these structures, while silicon nitride (SiN) waveguide could be a promising alternative to Si waveguide. This paper studies an integration approach between passive SiN waveguide and active Ge/SiGe multiple quantum wells (MQWs) optoelectronic modulators. Photocurrent measurements at different bias voltages demonstrated strong optical modulation within the O-band wavelength (1.26 – 1.36 μm) from Ge/SiGe MQWs, while 3D-FDTD calculations confirm a compact and efficient integration with SiN waveguide on Si wafer.

1. Introduction

Silicon (Si) photonics [1] has attracted much attention to enable a new generation of integrated low-power and low-cost photonic components through the well-established CMOS microelectronics technology. The high index contrast between Si and silicon dioxide (SiO_2) is ideal to shrink the footprint of optical devices and circuitries based on Si on insulator (SOI) waveguide. High performance active and passive photonic components have been demonstrated on the SOI waveguide platform [2]. Nevertheless for future telecommunication applications, the large refractive index contrast between Si and SiO_2 , high thermo-optical coefficient, and high optical nonlinearity of Si at 1.55 μm could pose a serious challenge for future dense wavelength division multiplexing (WDM) system. In other words, power durability, temperature stability, and phase errors due to technological robustness could hinder reliable WDM implementation on SOI platform.

Silicon nitride (SiN) waveguide could be studied as a promising alternative to Si waveguide. The refractive index of SiN is low enough to provide good fabrication tolerance and still high enough to obtain a compact photonic circuit. Moreover, SiN thermo-optical coefficient and optical nonlinearity are much less significant than those of Si. Previous works focused on integration of such passive SiN component with active Germanium (Ge) optoelectronic components such as Ge photodetector through Si waveguides on SOI wafer [3-4]. This paper studies a new integration approach between passive SiN waveguide and Ge/SiGe multiple quantum wells (MQWs) optoelectronic modulators. Photocurrent measurements at different bias voltages demonstrated strong optical modulation within the O-band telecommunication wavelength (1.26 – 1.36 μm) from Ge/SiGe MQWs; while, 3D-FDTD calculations confirm a compact and efficient integration with SiN waveguide through butt coupling approach on Si wafer, which we also briefly discussed in [5].

2. O-band optical modulation from Ge/ $\text{Si}_{0.15}\text{Ge}_{0.85}$ MQWs

In this paper, we developed an O-band optical modulation from Ge/SiGe MQWs by simply decreasing the quantum well thickness while keeping a constant material composition as those operating in the E-band wavelength regions. This approach is suitable for future WDM applications as it significantly relaxes fabrication complexity of Ge/SiGe MQW optical modulators operating at different wavelengths. In other words, the same Ge concentration could be employed to realize an optical modulator over a large wavelength range via varying only the QWs thickness, which could be achieved simultaneously across the wafer by using, for example, the local loading effect [6]. The MQWs were grown by low-energy plasma-enhanced chemical vapor deposition (LEPECVD) [7]. 20 periods of 6.5-nm-thick Ge QWs sandwiched between 10-nm-thick $\text{Si}_{0.15}\text{Ge}_{0.85}$ barriers were grown at a rate of 1 nm/s. The MQWs were embedded in a 35 nm $\text{Si}_{0.1}\text{Ge}_{0.9}$ spacer layers, a top 100-nm-thick $\text{Si}_{0.1}\text{Ge}_{0.9}$ phosphorous-doped n-type contact, and a bottom 300-nm-thick $\text{Si}_{0.1}\text{Ge}_{0.9}$ boron-doped p-type contact. The whole MQW stack is coherent with respect to a relaxed 300-nm-thick $\text{Si}_{0.1}\text{Ge}_{0.9}$ layer obtained via a graded buffer on Si wafer. Spectral photocurrent measurements were performed to evaluate material characteristics and device performance from a 50 μm diameter surface-illuminated diode, which was fabricated using standard ultraviolet (UV) lithography, dry etching, and metallization processes. A scanning electron microscopy (SEM) image of the 20 periods of QWs and an optical microscope image of the fabricated Ge/SiGe MQW surfaced-illuminated diode are shown in Fig. 1(a) and (b) respectively.

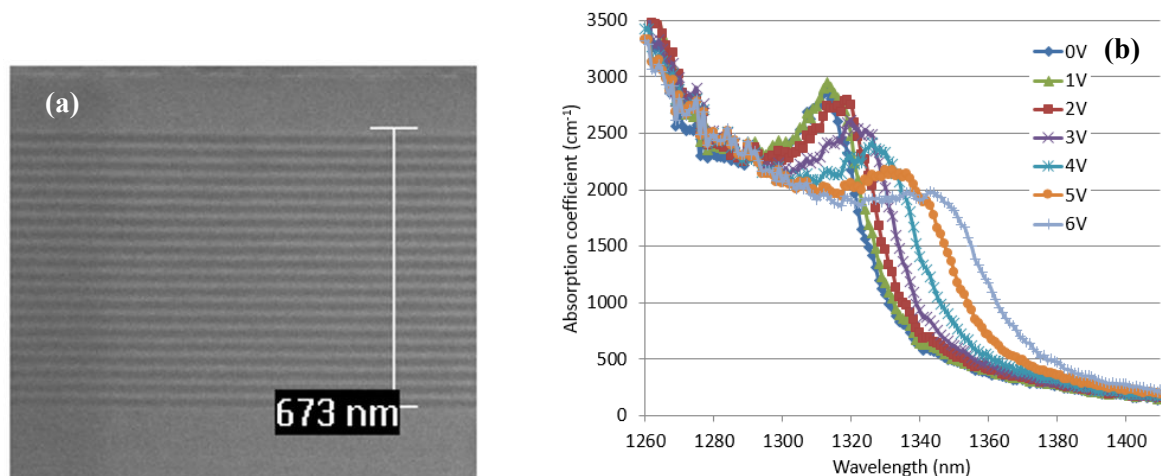


Figure 1. (a) SEM image of Ge/SiGe MQWs. (b) Absorption spectra from the photocurrent measurement at different reverse bias voltages. The excitonic $\text{HH1-c}\Gamma_1$ transition and strong QCSE were clearly observed within the O-band wavelength range (1260 – 1360 nm).

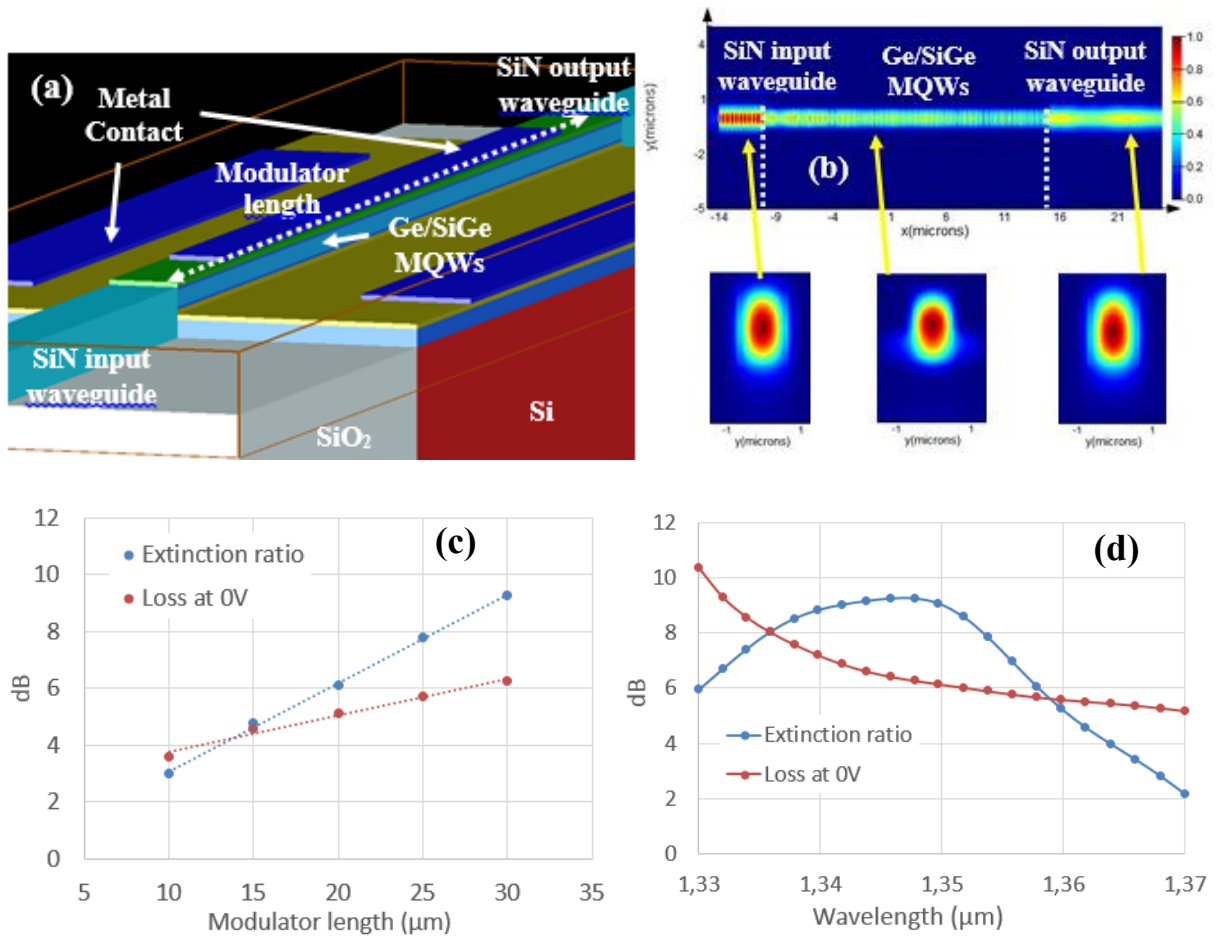


Figure 2. (a) Schematic view of the integration scheme between the passive SiN waveguide and the active Ge/SiGe QCSE modulator using butt coupling approach. (b) A top-view optical propagation and optical cross section profiles from input SiN waveguide via Ge/SiGe MQWs to the output waveguide. The extinction ratio and insertion loss evaluated from 3D-FDTD simulation (c) at different modulator lengths for $\lambda = 1.34 \mu\text{m}$ and (d) at different wavelengths for the modulator length of $30 \mu\text{m}$.

3. Silicon Nitride Waveguide-integrated optical QCSE modulator

We investigate the integration scheme between the passive SiN waveguide and the active Ge/SiGe QCSE modulator using butt coupling approach as in Fig. 2. Rigorous 3D-FDTD simulations were performed based on the experimentally-obtained values of absorption coefficients at different electrical bias voltages as reported in the section 2. As in Fig. 2(a), the simulated structure consisted of a $1.25\text{-}\mu\text{m}$ -wide $1\text{-}\mu\text{m}$ -thick input strip SiN waveguide coupled with a $1.25\text{-}\mu\text{m}$ -wide Ge/SiGe MQWs waveguide embedded in a p-i-n with a top and a lateral bottom contact metal of aluminum (Al). At the output part, another $1.25\text{-}\mu\text{m}$ -wide $1\text{-}\mu\text{m}$ -thick input strip SiN waveguide was coupled also with Ge/SiGe MQWs. The Ge/SiGe MQWs absorption properties at different bias voltages was obtained from the experiments in the section 2. The green part indicates a 100-nm -thick $\text{Si}_{0.1}\text{Ge}_{0.9}$ phosphorous-doped n-type layer and the yellow part is a 200-nm -thick $\text{Si}_{0.1}\text{Ge}_{0.9}$ boron-doped p-type layer. The Ge/SiGe MQWs structure sits on a 360-nm -thick $\text{Si}_{0.1}\text{Ge}_{0.9}$ buffer growth directly on Si [9].

From 3D-FDTD simulation, the extinction ratio and insertion loss were evaluated at different modulator lengths (the length of the Ge/SiGe MQW region) between the bias voltage of 0 and 6 V at the light wavelength of 1340 nm , which is the optimal operating point of the fabricated sample as in Fig.

1(b). The optimal operating wavelength can be shifted to 1310 nm by simply decreasing the quantum well width further [10, 11]. Fig. 2(b) shows a top-view optical propagation and optical cross section profiles of the 3D-FDTD simulation from input SiN waveguide via Ge/SiGe MQWs to the output waveguide, which confirming a low loss butt coupling integration. As in Fig. 2(c) at the optical wavelength of 1.346 μm , with only the modulator length of 30 μm , an extinction ratio of 9.3 dB was obtained with an insertion loss of less than 6.3 dB, which already included the background loss due to Ge/SiGe absorption, N-type and P-type layer absorption, possible metal absorption, and the coupling loss between the input and output SiN waveguides and the Ge/SiGe modulator. Fig. 2(d) reports wavelength dependence of the extinction ration and optical loss obtained from the 30- μm -long modulator from the 3D-FDTD simulation; the waveguide-integrated structure is found to have extinction ratio values more than the operating optical loss for over 20 nm spectral width.

Acknowledgments

Marie Curie International Outgoing Fellowships through Grant Agreement No. PIOF-GA-2013-629292 MIDEX.

References

- [1] Kimerling L C, Kwong D L and Wada K, 2014 Scaling computation with silicon photonics *MRS Bulletin* **39**, 687-695
- [2] Marris-Morini D, Virot L, Baudot C, Fédéli J M, Rasigade G, Perez-Galacho D, Hartmann J M, Olivier S, Brindel P, Crozat P, Bœuf F and Vivien L, 2014 A 40 Gbit/s optical link on a 300-mm silicon platform *Optics Express* **22** 6674-6679
- [3] Doerr C R, Chen L, Buhl L L and Chen Y, 2011 Eight-Channel SiO/SiN Si/Ge CWDM Receiver *IEEE Photonics Technology Letters* **23** 1201-1203
- [4] Piels M, Bauters J F, Davenport M L, Heck M J R and Bowers J E 2014 Low-Loss silicon nitride AWG demultiplexer heterogeneously integrated with hybrid III–V/Silicon photodetectors *Journal of Lightwave Technology* **32** 817-823
- [5] Zhang Z, Chaisakul P, Yako M, Kan J, Yamada K, Tsuchizawa T, Fukuda H, Marris-Morini D, Vivien L, Kawai N and Wada K 2015 A study of physical vapor deposition silicon nitride for dense wavelength division multiplexing on silicon wafer *SPIE Microtechnologies*, Barcelona, Spain, May 4 – 6
- [6] Kamins T I 1993 Pattern sensitivity of selective Si_{1-x}Ge_x chemical vapor deposition: pressure dependence *J. Appl. Phys.* **74** 5799-5802
- [7] Isella G, Chrastina D, Rössner B, Hackbarth T, Herzog H J, König U and von Känel H 2004 Low-energy plasma-enhanced chemical vapor deposition for strained Si and Ge heterostructures and devices *Solid State Electron.* **48** 1317
- [8] Chaisakul P, Marris-Morini D, Isella G, Chrastina D, Le Roux X, Gatti E, Edmond S, Osmond J, Cassan E and Vivien L 2010 Quantum-confined Stark effect measurements in Ge/SiGe quantum-well structures *Opt. Lett.* **35** 2913–2915
- [9] Rouifed M S, Marris-Morini D, Chaisakul P, Frigerio J, Isella G, Chrastina D, Edmond S, Le Roux X, Coudeville J R, Bouville D and Vivien L 2014 Advances toward Ge/SiGe quantum-well waveguide modulators at 1.3 μm *IEEE. J. Sel. Top. Quantum Electron.* **20** 3400207
- [10] Chaisakul P, Frigerio J, Marris-Morini D, Vakarin V, Chrastina D, Isella G and Vivien L 2014 O-band quantum-confined Stark effect optical modulator from Ge/Si_{0.15}Ge_{0.85} quantum wells by well thickness tuning *J. Appl. Phys.* **116** 193103
- [11] Chaisakul P, Marris-Morini D, Frigerio J, Chrastina D, Rouifed M-S, Cecchi S, Crozat P, Isella G, Vivien L 2014 Integrated germanium optical interconnects on silicon substrates *Nat. Photon.* **8** 482–488